Electronic Supplementary Material (ESI) for Journal of Materials Chemistry C.

Supporting Information

Gas-Sensing Performance of Core-shell SnO_2-based Chemiresistive MEMS Sensor for H_2S Detection under Vacuum

Wenbo Pi[a, ‡], Xi Chen[a,‡], Qiuyun Fu[a], Zixiao Lu[b], Honglang Li[b], Zaiqi Tang[c],and Wei Luo[a,d]*

[a]*School of Integrated Circuits, Huazhong University of Science and Technology, Wuhan 430074, PR China*

[b]*CAS Center for Excellence in Nanoscience, National Center for Nanoscience and Technology, Beijing 100190, PR China*

[c]*Sysmo Technologies Co., LTD, Beijing 100020, PR China*

[d]*Research Institute of Huazhong University of Science and Technology in Shenzhen, Shenzhen 518000, PR China*.

[‡]*These authors contributed equally to this work.*

**E-mail: luowei@mail.hust.edu.cn*

Characterization of silver interdigital electrode SnO_2 gas sensor after introducing H_2S gas.

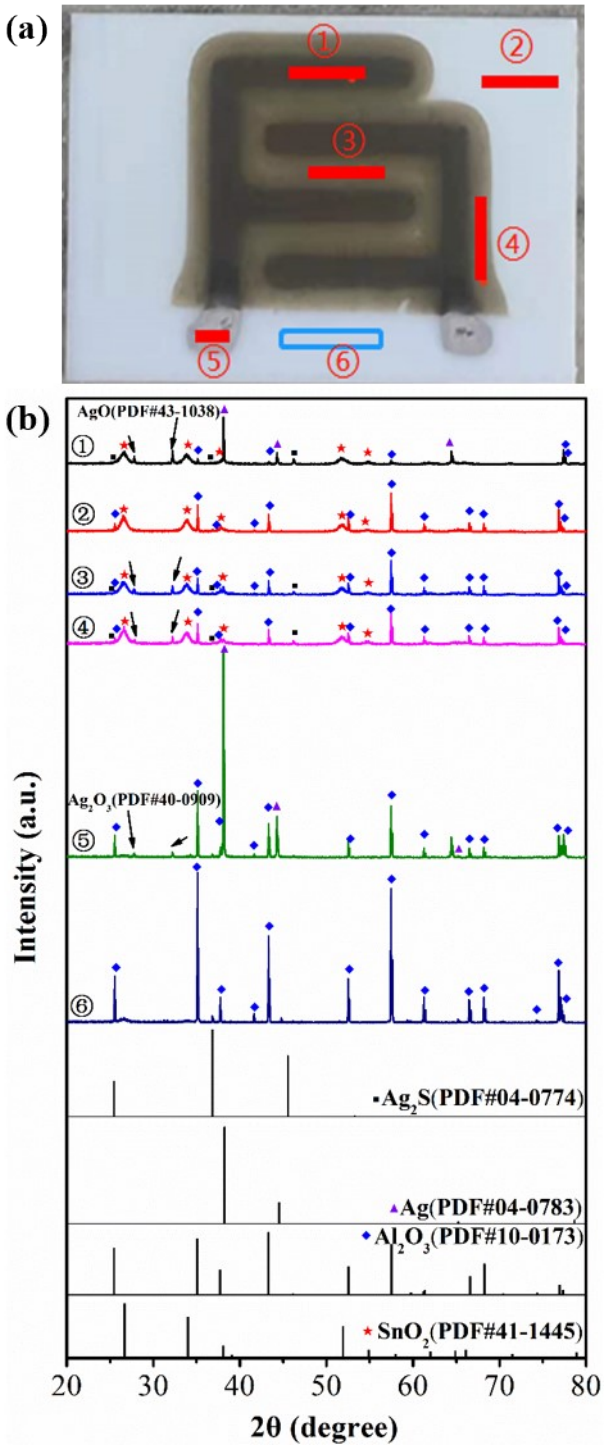

Figure S1. (a) Photo of the silver interdigital electrode SnO_2 gas sensor after introducing H_2S gas at ambient temperature and pressure, (b) Micro-area XRD pattern of the silver interdigital electrode SnO_2 gas sensor exposed to H_2S gas.

When 1 ppm of H_2S gas was introduced to the SnO_2 gas sensor through the silver interdigital electrode, an exponential decrease in the resistance of the SnO_2 gas sensor was observed. It is noteworthy that after the gas sensing reaction, the SnO_2 sensitive

film above and around the silver interdigital electrode of the gas sensor turned brownish-yellow, while the color of the SnO_2 sensitive film away from the silver interdigital electrode remained unchanged, as shown in Figure S1(a). The phase composition of each part of the silver interdigital electrode SnO_2 gas sensor exposed to H_2S was studied using a micro-area X-ray diffractometer, and the XRD spectrum is shown in Figure S1. The results showed that there were small amounts of Ag_2O and Ag_2S around the Ag electrode, which implied that there were two possible processes for this gas-sensitive reaction: one is the direct reaction between Ag and H_2S gas to generate Ag_2S, another is the reaction between the Ag_2O and H_2S. Both gas-sensitive processes are expected to be applied in the detection of H_2S under low-temperature and high-vacuum conditions.

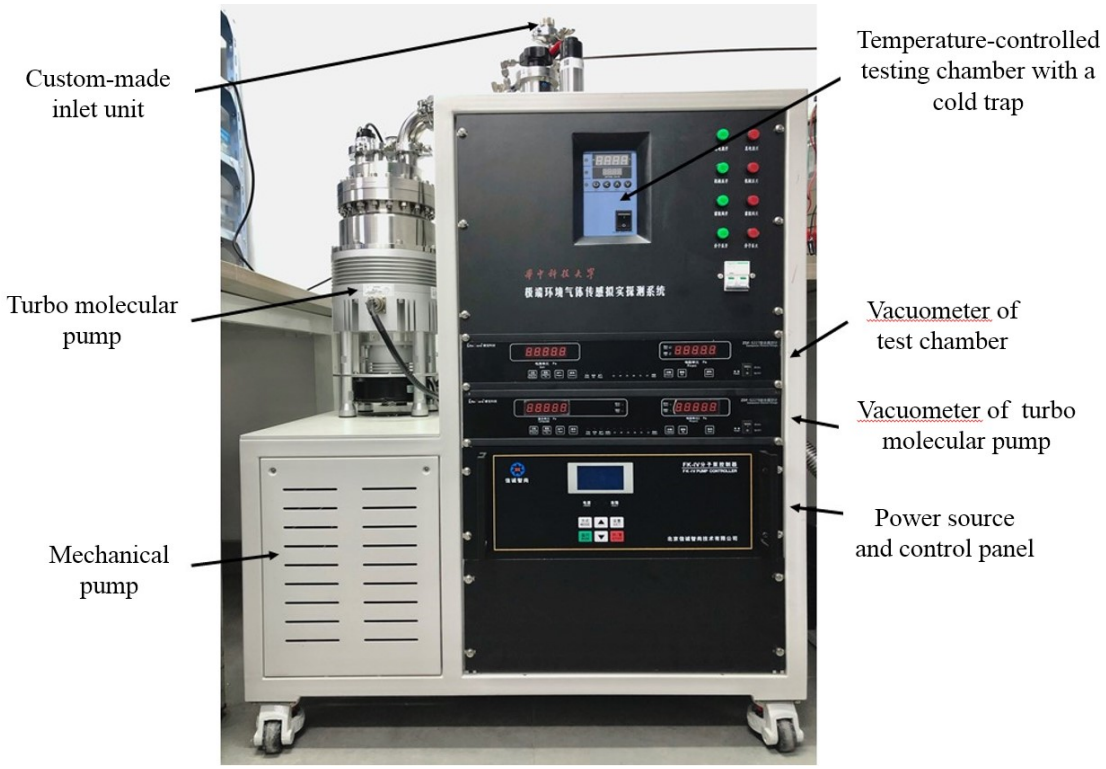

Figure S2. Gas sensor test system under low temperature and high vacuum

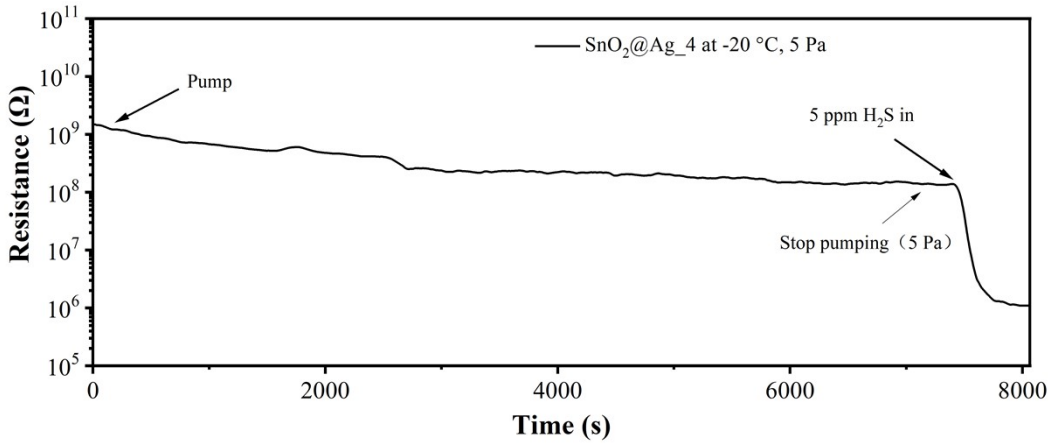

Figure S3. The response curve of SnO_2@4Ag gas sensor to 5 ppm H_2S in a low-temperature and low-vacuum condition (-20 °C, 5 Pa)

Then, SnO_2@4Ag gas sensor was tested for its gas sensing performance towards 5 ppm of H_2S gas in a low-temperature and low-vacuum test system (−20 °C, 5 Pa). The experimental results, as shown in Figure S3, indicated that upon injecting 5 ppm of H_2S gas into the system, the resistance of the SnO_2@4Ag gas sensor immediately decreased, and the response value reached above 100, indicating its capability of detecting H_2S gas in such a low-temperature and low-vacuum environment (−20 °C, 5 Pa).

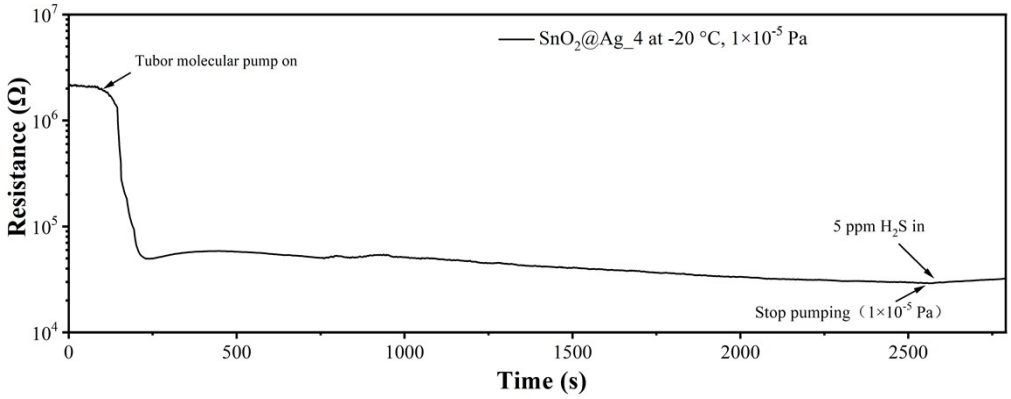

Figure S4. The response curve of SnO_2@Ag_4 gas sensor to 5 ppm H_2S in a low-temperature and high-vacuum condition (-20 °C, 1×10^{-5} Pa)

As shown in Figure S4, upon injecting 5 ppm of H_2S gas into the test system (−20 °C, 1×10^{-5} Pa), the SnO_2@Ag_4 gas sensor showed no response, and its resistance only had a slightly increasing trend, which was completely different from the experimental phenomenon observed under low-temperature and low-vacuum conditions.

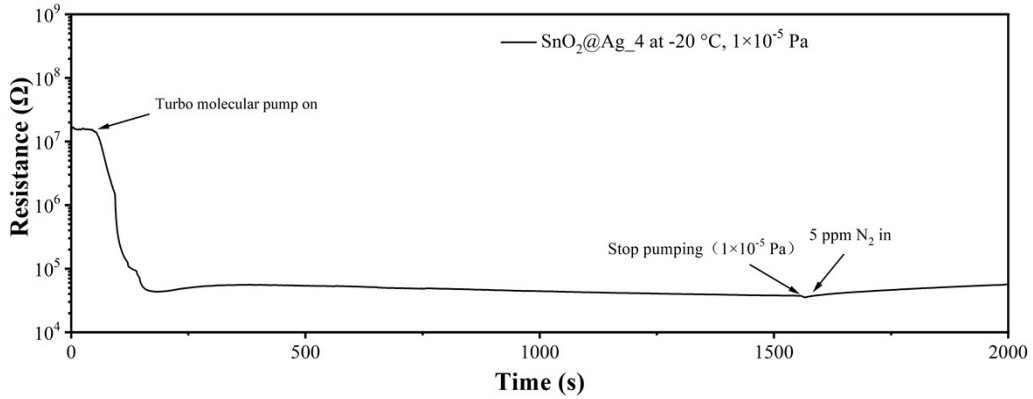

Figure S5. The response curve of SnO_2@Ag_4 gas sensor to 5 ppm N_2 in a low-temperature and high-vacuum condition (-20 °C, 1×10^{-5} Pa)

As shown in Figure S5, upon introducing an equal amount of N_2, the resistance of the sensor also showed a slightly increasing trend, which was consistent with the experimental phenomenon observed in Figure S4. This indicates that under high-vacuum conditions, SnO_2 and Ag did not react with H_2S.

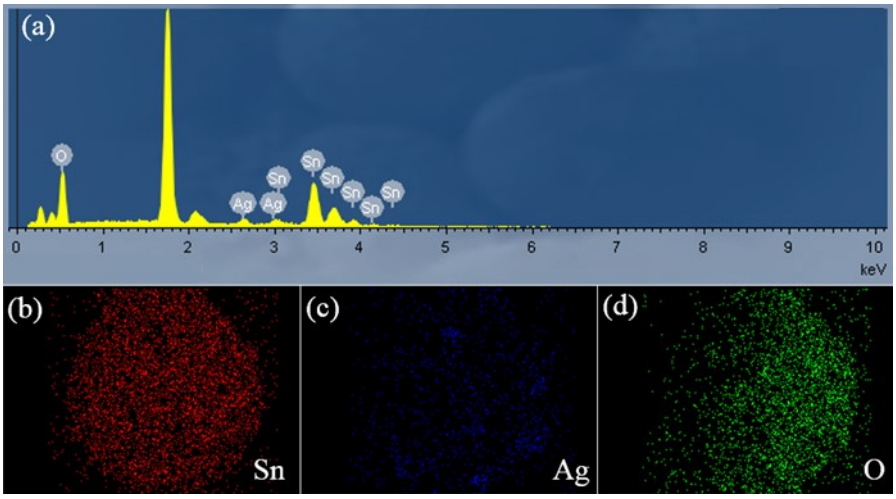

Figure S6. (a) EDS spectra, and (b-d) elemental mapping of SnO_2@Ag_2O_2

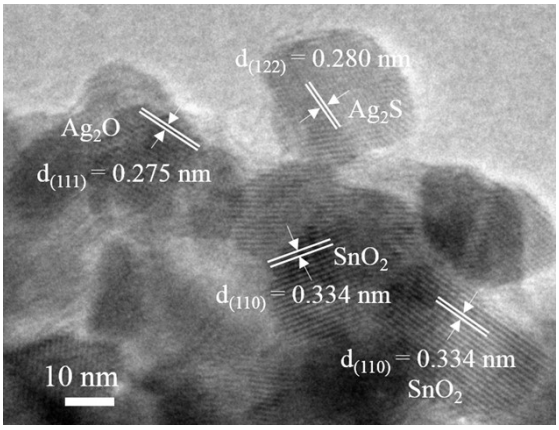

Figure S7. High-resolution TEM image of SnO_2@Ag_2O_2 after exposure to H_2S

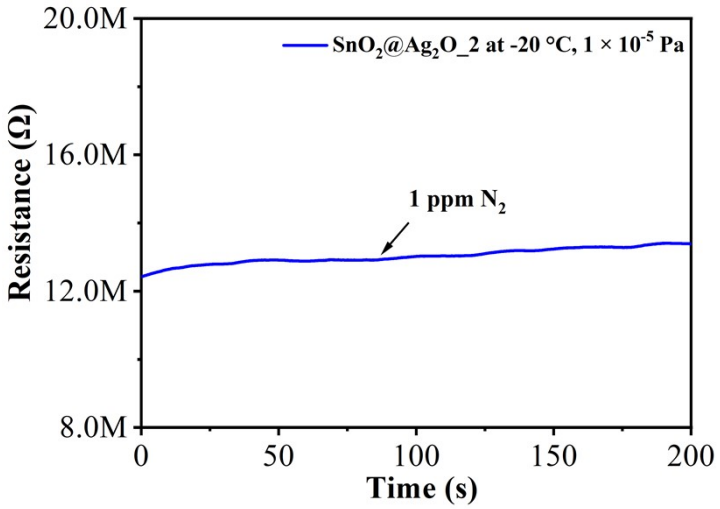

Figure S8. Gas sensing response curve of SnO_2@Ag_2O_2 gas sensor towards with 0.4 mL N_2

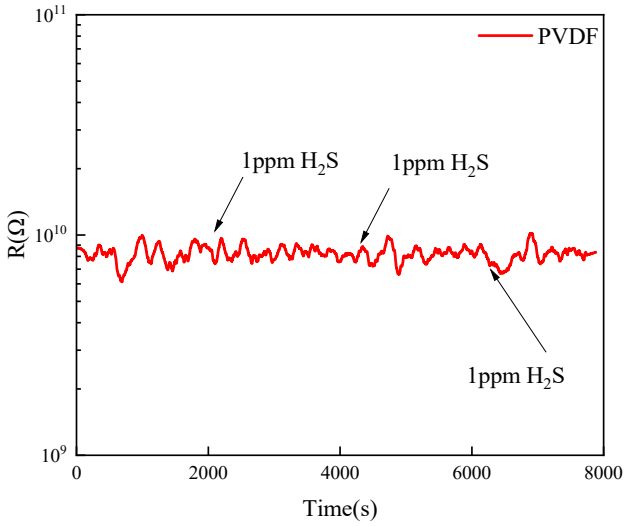

Figure S9 The PVDF for H_2S gas detection under vacuum (1×10^{-5} Pa).

Table 1

Method	Spacecraft Model	Mass (kg)	Power (W)	Size (cm × cm × cm)	Sensitivity and Limitation
Mass Spectrometry	Phoenix Mars Lander[1]	5.7	13	24 × 23× 18	0.7 to 4, 7–35, 14–70 and 28–140 amu;H_2O、CO_2、H_2、O_2、NH_3、SO_2
	Huygens[2]	17.3	28	Φ19.8 × 47	2～ 141 amu
	Pioneer Venus project[3]	3.81	12	Φ 0.2 × 7.5	1-64 amu; CO CO_2 N_2
Visible Spectrometer	LADEE[4]	3.6	13	-	Mean noise-equivalent power ~45 R/nm
Our method		<10g	<1 W	0.5	H_2S, 100 pb

1. *Journal of the American Society for Mass Spectrometry Volume 19, Issue 10, October 2008, Pages 1377-1383*
2. *Niemann, H. B., Atreya, S. K., Bauer, S. J., et al. (2003). The gas chromatograph mass spectrometer for the Huygens probe. In The Cassini-Huygens Mission (pp. 553-591). Dordrecht: Springer Netherlands*
3. *Hoffman, J. H., Hodges, R. R., Wright, W. W., et al. (1980). Pioneer Venus sounder probe neutral gas mass spectrometer. IEEE Transactions on Geoscience and Remote Sensing, 18(1), 80-84.*
4. *Elphic, R.C. et al. (2015). The Lunar Atmosphere and Dust Environment Explorer Mission. In: Elphic, R., Russell, C. (eds) The Lunar Atmosphere and Dust Environment Explorer Mission (LADEE). Springer, Cham. Space Science Reviews*